Structure of ice crystallized from supercooled water

Tamsin L. Malkin[a], Benjamin J. Murray[a,1], Andrey V. Brukhno[b], Jamshed Anwar[c], and Christoph G. Salzmann[d,2]

[a]Institute for Climate and Atmospheric Science, School of Earth and Environment, University of Leeds, Woodhouse Lane, Leeds LS2 9JT, United Kingdom; [b]Centre for Molecular Nanoscience, University of Leeds, Woodhouse Lane, Leeds LS2 9JT, United Kingdom; [c]Institute of Life Sciences Research, University of Bradford, Bradford BD7 1DP, United Kingdom; and [d]Department of Chemistry, Durham University, South Road, Durham DH1 3LE, United Kingdom

Edited by T. C. Lubensky, University of Pennsylvania, Philadelphia, PA, and approved November 22, 2011 (received for review August 18, 2011)

The freezing of water to ice is fundamentally important to fields as diverse as cloud formation to cryopreservation. At ambient conditions, ice is considered to exist in two crystalline forms: stable hexagonal ice and metastable cubic ice. Using X-ray diffraction data and Monte Carlo simulations, we show that ice that crystallizes homogeneously from supercooled water is neither of these phases. The resulting ice is disordered in one dimension and therefore possesses neither cubic nor hexagonal symmetry and is instead composed of randomly stacked layers of cubic and hexagonal sequences. We refer to this ice as stacking-disordered ice I. Stacking disorder and stacking faults have been reported earlier for metastable ice I, but only for ice crystallizing in mesopores and in samples recrystallized from high-pressure ice phases rather than in water droplets. Review of the literature reveals that almost all ice that has been identified as cubic ice in previous diffraction studies and generated in a variety of ways was most likely stacking-disordered ice I with varying degrees of stacking disorder. These findings highlight the need to reevaluate the physical and thermodynamic properties of this metastable ice as a function of the nature and extent of stacking disorder using well-characterized samples.

The freezing of water to ice is of fundamental importance in both nature and technology. Yet the structure of the phase of ice that initially crystallizes is poorly understood. Freezing is thought to follow Ostwald's rule of stages, which states that a metastable phase crystallizes initially, which may later transform to the stable phase (1). In the case of ice crystallized from liquid water at ambient pressure, the metastable phase has been previously identified as cubic ice (ice I_c) (2–4). This metastable phase is thought to persist in the coldest regions of Earth's atmosphere where temperatures fall below 200 K (2, 4–8). It is also observed in biological tissues during cryopreservation where it is considered to be benign to the tissue, unlike hexagonal ice (ice I_h) (9, 10). However, in many situations it will rapidly transform into the stable hexagonal phase, especially at common environmental temperatures (3). Even though it may be short-lived, it can have a lasting effect. For example, in the atmosphere, the transient presence of the metastable phase is thought to modify the shape of snowflakes (11) and may lead to substantial changes in ice-particle concentrations in cold cirrus clouds (5).

In both modifications of ice I, ice I_h, and ice I_c, the water molecules form layers consisting of six-membered puckered rings. The difference between ice I_h and ice I_c lies in the stacking of these layers. In the case of ice I_h, each layer is a mirror image of the previous layer, which results in an overall structure with hexagonal symmetry. In ice I_c, on the other hand, each successive layer is shifted a distance equal to half the diameter of a six-membered ring. In the resulting structure, the oxygen atoms are arranged in the same way as carbon atoms in the cubic lattice of diamond (12, 13).

It has been noted in the past that the diffraction patterns of metastable ice crystallized from bulk water droplets are not in agreement with a perfect cubic crystal structure (e.g., refs. 3, 4, and 14). In fact, ice referred to as cubic ice, which was generated by recrystallization from high-pressure phases (15–17), by freezing of confined water in mesopores (18), and by warming amorphous ice (19), is also not perfect cubic ice.

It is well known that crystallites with periodic stacking sequences can contain stacking faults where, for example, a cubic sequence might "accidentally" appear in a predominantly hexagonal structure. This kind of disorder is common in clays, metals, and zeolites (20). The stacking faults interrupt the periodicity of the crystal in the direction of the stacking, although the crystal may remain well ordered in the other two dimensions. A number of authors have suggested that the noncubic features in metastable ice can be explained by stacking faults (3, 14, 17, 21). More recently, Hansen et al. (16, 22) quantified the stacking faults in what they referred to as cubic ice, which was recrystallized from ice V and IX. In contrast, Morishige et al. (18) refer to ice in mesopores as cubic ice, but suggest that it is in fact small crystallites of hexagonal ice with growth faults.

In this paper, we elucidate and characterize the structure of the metastable phase of ice I that crystallized from droplets of supercooled water and quantify the stacking disorder by means of stacking probabilities. We also use Monte Carlo simulations to probe crystallization of ice at a molecular level. Both the experimental and computational data support the thesis that stacking disorder is a general feature of ice formation from supercooled water.

Results and Discussion

X-Ray Diffraction Study of Frozen Water Droplets. In order to determine the crystal structure of ice that crystallized homogeneously from supercooled water, water droplets were suspended in an oil matrix by emulsification, and the phase of ice that formed was monitored with X-ray diffraction (see *Methods*).

Comparison of the diffraction pattern of frozen 0.9-μm droplets that froze around 232 K (Fig. 1*A*) with the calculated pattern for ice I_h (Fig. 1*B*) reveals that the characteristic hexagonal peaks at about 26°, 34°, and 61° 2θ, which are the 101, 102, and 203 peaks of ice I_h, are absent, whereas the remaining peak intensities are inconsistent with ice I_h. Our diffraction pattern is similar to numerous patterns published in the literature, which have been identified as ice I_c (e.g., refs. 3, 4, 19, and 23). However, comparison of the experimental pattern with the numerically calculated pattern for ice I_c (Fig. 1*C*) reveals obvious discrepancies. The experimental pattern has a strong peak at approximately 23° (corresponding to the 100 peak of ice I_h) and the region between approximately 23° and 26° is elevated above the baseline; both of these features are incompatible with cubic symmetry. Moreover, the relative peak intensities of the three primary peaks of ice I_c are a poor match to the experimental

Author contributions: B.J.M., A.V.B., and J.A. designed research; T.L.M., A.V.B., and C.G.S. performed research; T.L.M. and A.V.B. analyzed data; and T.L.M., B.J.M., A.V.B., J.A., and C.G.S. wrote the paper.

The authors declare no conflict of interest.

This article is a PNAS Direct Submission.

Freely available online through the PNAS open access option.

[1]To whom correspondence should be addressed. E-mail: B.J.Murray@Leeds.ac.uk.

[2]Present address: Department of Chemistry, University College London, 20 Gordon Street, London WC1H 0AJ, United Kingdom.

This article contains supporting information online at www.pnas.org/lookup/suppl/doi:10.1073/pnas.1113059109/-/DCSupplemental.

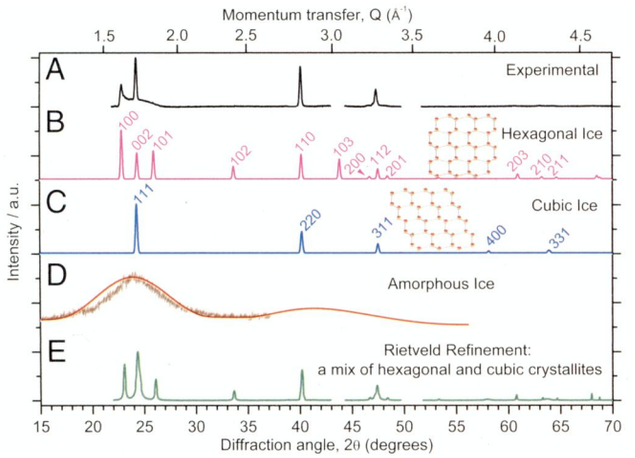

Fig. 1. Experimental and calculated X-ray diffraction patterns. (*A*) An experimental diffraction pattern for water droplets (volume median diameterdiameter = 0.9 μm) that froze homogeneously with a median freezing temperature of 231.7 ± 1 K on cooling at 30 K min^{-1} recorded at *ca.* 173 K. (*B* and *C*) Simulated diffraction patterns using DIFFaX of fully ordered ice I_h and ice I_c, respectively. (*D*) The literature diffraction patterns of amorphous ice from Dowell and Rinfret (23) below 113 K (bright red) and Shilling et al. (19) at 90 K (dark red). (*E*) The result of a Rietveld refinement to the experimental pattern, assuming a mixture of well-crystallized ice I_c and ice I_h. The gaps in the experimental pattern correspond to diffraction peaks from the sample support.

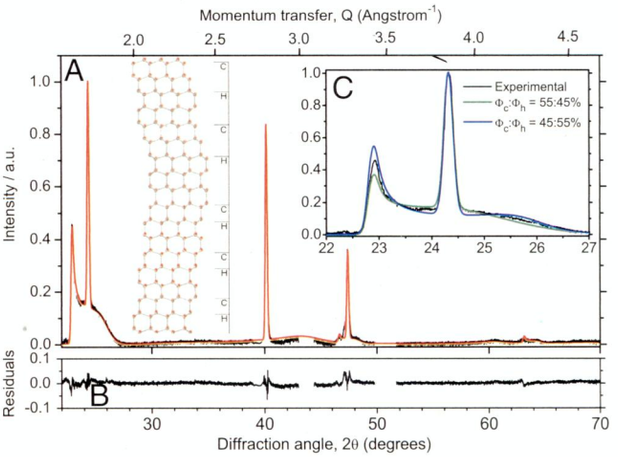

Fig. 2. (*A*) Comparison of the experimental X-ray diffraction patterns of frozen water droplets (d_{vm} ~ 0.9 μm) and a DIFFaX model prediction for random stacking sequences ($\Phi_c:\Phi_h$ = 50%:50%). (*B*) The residuals of experimental diffraction pattern minus model prediction. (*C*) The DIFFaX prediction for stacking probabilities $\Phi_c:\Phi_h$ = 45%:55% and 55%:45%, which are less consistent with the data. We implicitly assume that the stacking ratio is identical for each droplet in these calculations.

pattern, and the high angle peaks (*ca.* 58° and 64° corresponding to the 400 and 331 peaks of ice I_c) are absent. In the past, it has been suggested that crystallization of amorphous ice on heating is incomplete, resulting in a mixture of crystalline and amorphous ice (23, 24). Comparison of our experimental pattern (Fig. 1*A*) with amorphous patterns from the literature (Fig. 1*D*) clearly shows that our sample does not contain amorphous ice. It is also apparent from a Rietveld refinement (Fig. 1*E*) that the metastable material is not a simple phase mixture of crystallites of ice I_c and ice I_h. In summary, it is clear from these diffraction patterns that the ice, which crystallizes from supercooled water, is neither ice I_c, ice I_h, nor a mixture of distinct phases.

The experimental diffraction pattern of ice from supercooled water is in fact consistent with ice that contains stacking disorder. For perfectly ordered crystals, diffraction intensity in reciprocal space is only observed at certain points, whose locations are defined by the integral h, k, and l Laue indices. The presence of stacking disorder in layered materials can, however, result in the appearance of "streaks" in reciprocal space, which means that diffraction intensity is found along continuous values of the index l if the layers are oriented perpendicular to the crystallographic c axis. Consequently, asymmetric peak broadening can be observed in powder diffraction (25). Only Bragg peaks where $(h-k)/3$ is not integral are affected by the stacking disorder (25). For example, the 100, 101, and 102 peaks are all broadened or even absent in our experimental pattern. Peaks with greater values of l are more susceptible to stacking disorder (26), which is also consistent with our experimental patterns. In order to quantitatively characterize the structure of the ice formed in these experiments, we employed the DIFFaX (Diffracted Intensities from Faulted Xrystals) computer program (20), for calculating powder diffraction patterns of crystals containing stacking disorder (see *Methods* for details).

In Fig. 2, we compare the pattern of frozen 0.9-μm droplets with the DIFFaX prediction based on the assumption that, as the ice grows, it randomly switches between hexagonal and cubic sequences [i.e., the probabilities of an emerging sequence changing (or faulting) from cubic to hexagonal Φ_h or from hexagonal to cubic Φ_c are equal and also independent of the previous sequences; $\Phi_c:\Phi_h = 50:50\%$; see *Methods* for a full explanation]. The match between the theoretically predicted and experimentally obtained patterns is very good (Fig. 2; $\chi^2 = 0.007$). In contrast, Fig. 2*C* shows the DIFFaX result for $\Phi_c:\Phi_h = 45:55\%$ and 55:45%, both of which exhibit pronounced deviations ($\chi^2 = 0.019$). In addition, DIFFaX allows us to rule out the possibility of fault clustering or memory effects (further discussed in the *Methods* and *SI Text*). We conclude that ice crystallized homogeneously from supercooled water is ice I, in which cubic and hexagonal stacking sequences are randomly arranged. A more accurate name for this material would be stacking-disordered ice I, for which we suggest the shorthand ice I_{sd}. In future studies of ice I_{sd} the stacking probability in terms of $\Phi_c:\Phi_h$ should be quoted.

Monte Carlo Simulations of Water Freezing. Independent evidence for the ice I_{sd} structure comes from computer simulations that yield molecular resolution and bring direct insights into molecular processes of ice crystallization. Homogeneous nucleation of ice occurs on timescales that are generally not accessible by brute-force simulation, and here we employed advanced Monte Carlo (MC) simulations in which we efficiently direct and enhance ice growth from supercooled water at 220 K for a periodic system comprising 2,880 TIP4P model water molecules (note that the melting temperature for this model is 232 K). An essential issue with such simulations is that one must ensure that the methodology does not favor a particular structure or phase (27), and to this end, we used the order parameters previously developed and verified by Brukhno et al. (28).

The striking observation from our simulations is that, during crystallization of ice I, the emerging ice layers randomly switch between cubic and hexagonal sequences. This process is illustrated in Fig. 3, where a simulation snapshot of the developing ice crystal structure is presented, and also in Fig. 4, where the ratio, $\Phi_c:\Phi_h$, is plotted against the (effective) MC time for several trajectories. In general, the ice structure formed in our simulations is always disordered in terms of the stacking sequence, with inevitable fluctuations in $\Phi_c:\Phi_h$ because of the relatively small number of molecules in the simulation box. Other numerical studies of growth on an ice surface (29, 30) and nucleation in the subsurface region (31) also confirm the propensity of ice to grow in a stacking-disordered manner. The presented simulation results are consistent with our analysis of the experimental data

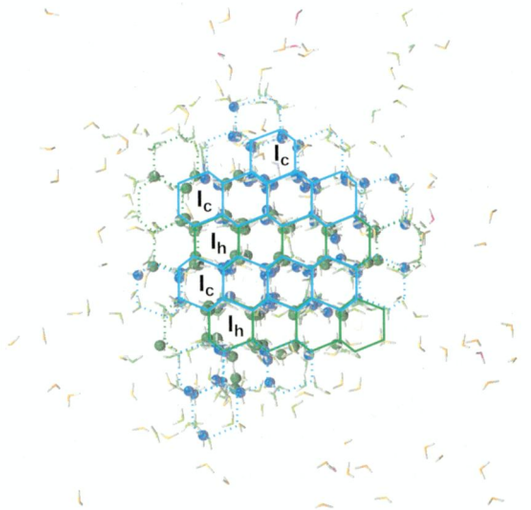

Fig. 3. Snapshot of ice crystal structure at 220 K as observed in Monte Carlo molecular simulations. Highly correlated oxygen atoms (i.e., in a well-ordered structure) that form the ice structure are shown as spheres, whereas molecules that are less correlated are indicated with sticks, and uncorrelated water molecules are not shown. O atoms in the ice I_h environment are shown in green, and those in the ice I_c configuration are blue. The cubic and hexagonal stacking are highlighted with blue and green lines, respectively, dotted lines indicate the developing parts of the structure.

and strongly support the interpretation of the X-ray diffraction data.

Conclusions

Both the experimental diffraction patterns and the simulation data agree in that ice, which initially crystallizes from supercooled water, has neither purely cubic nor hexagonal structure, but is identified as stacking-disordered ice I. This finding offers a mechanistic insight into the crystallization of water. The evidence suggests that a stacking-disordered material forms more rapidly than either of the distinct phases and the process is probably dominated by kinetics.

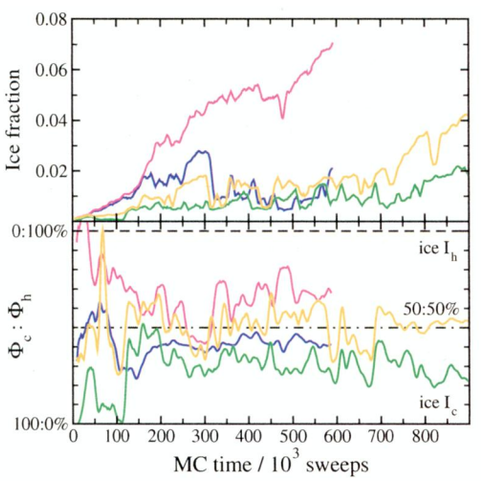

Fig. 4. Growth of ice crystals as a function of time and their stacking disorder in the Monte Carlo simulations. (*A*) The evolution of cluster size (expressed as ice fraction) with time at 220 K. (*B*) The evolution of the ratio of the stacking probability $\Phi_c : \Phi_h$ with MC time. $\Phi_c : \Phi_h$ is determined assuming no "memory" effect (i.e., $\Phi_h + \Phi_c = 100\%$; see *Methods*), hence Φ_c is equivalent to the percent of molecules in a cubic environment. MC time is the number of sweeps through the system, during each of which every molecule is given the opportunity to translate and rotate.

By definition, a crystalline solid is a material in which there is periodicity in all three dimensions. Ice I_{sd} is only ordered in two dimensions and is disordered in the direction of stacking of oxygen atom layers; hence it is unlikely to form macroscopic crystals of a distinct shape (habit). Ice I_c is expected to form cubes or octahedra, and ice I_h most often forms hexagonal plates and columns and underlie the familiar shape of snowflakes (32). The habit of single crystallites of ice I_{sd} is unknown, but they might be expected to have two smooth parallel faces corresponding to either the [0001] face of ice I_h or the [111] face of ice I_c (which are equivalent), but with the other sides poorly defined. Intriguingly, Lawson et al. (33) reported that more than 80% of the crystals they imaged in tropical cirrus were "quasi-spheroids" but with some flat edges. Recent results from 2D laser scattering probes also suggest that many ice crystals in cirrus and mixed-phase clouds are irregular and may have rough surfaces (34). Ice-particle shape and roughness has a profound impact on cloud radiative properties with moderately rough particles, reflecting nearly twice the solar radiation as smooth crystals (34). The role of stacking disorder in atmospheric crystals clearly needs to be investigated in detail.

Ice generated in different ways appears to have different stacking fault densities. Our study has established that the ice formed from supercooled water under atmospherically relevant conditions is fully stacking disordered (50%:50%), whereas ice recrystallized from the high-pressure phase ice V contains about 60% cubic sequences, and ice from ice IX contains about 42% cubic sequences at 175 K (16, 22). Also, Kuhs et al. (17) estimated that ice I_{sd} from ice II contained only a few percent of hexagonal sequences, although this should be reassessed with a quantitative model. The appearance of varying degrees of stacking disorder raises important questions about the validity and applicability of the physical data for so-called cubic ice in the literature, including thermodynamic quantities, such as heat capacity and vapor pressure as well as interfacial energies, optical constants, and spectroscopic properties. It is necessary to revisit many of these measurements using well-characterized ice in order to understand the relationship between stacking disorder and the physical properties of the ice I family. Such studies will underpin our understanding of ice formation and properties in a wide range of fields including the atmospheric sciences, cryobiology, glaciology, geophysics, engineering, and the planetary sciences (13).

An obvious question is whether well-ordered ice I_c can ever form. Although evidence from diffraction measurements is absent, crystals grown from water vapor at approximately 200 K can have a cubic habit (35) and 25% of crystals in the Antarctic stratosphere were solid cubes during one campaign (36). In addition, a halo at 28° from the sun has been photographed and is consistent with the rare presence of octahedral crystals of ice I_c in the atmosphere (37). Perhaps the dearth of hard evidence for the existence of well-ordered ice I_c indicates that it is rare and only forms under very specific conditions, which diffraction experiments have not yet accessed.

Methods

Sample Preparation. The experimental technique has been described previously (2, 3) and will only be briefly summarized here. For these experiments, pure water (18.2 MΩ) droplets were suspended in an oil matrix (10 wt % lanolin in mineral oil) and were agitated to make droplets of the desired size. The lanolin served as a surfactant and stabilized the emulsion. Droplets > 5 μm heat up during crystallization and partly anneal to the stable hexagonal phase (3). In contrast, very small droplets do not anneal to the stable phase. A diffraction pattern of 0.9-μm droplets cooled at 30 K min^{-1} is shown in Fig. 1*A*. These droplets froze with a median freezing temperature of 231.7 ± 1.0 K, consistent with the temperature of 232.2 K expected for homogeneous freezing under these conditions (38), showing that the presence of the oil and surfactant did not alter the nucleation kinetics.

Experimental Procedure. The X-ray diffractometer (Bruker D8 Advance) used in these experiments was configured in a standard reflection geometry and

was equipped with a Cu Kα X-ray source ($\lambda = 1.5418$ Å), a Vantec detector, and an Anton Paar TTK450 temperature-controlled stage. The sample holder was cooled by liquid nitrogen to 173 K at a rate of 30 K min^{-1}. The diffraction patterns were recorded with the sample under vacuum to prevent frosting and reduce heat transfer. In order to measure the temperature at which the water droplets homogeneously froze to ice, the diffraction angle of a strong reflection associated with both ice I_c and ice I_h (diffraction angle, $2\theta = 24°$) was continually monitored as the cell was cooled. Once at 173 K, the diffraction pattern of the sample between $2\theta = 20$ and 70° was recorded. This range covered all of the strong ice I_c and ice I_h reflections, and selected examples of the resulting patterns are illustrated in Figs. 1 and 2 and *SI Text*.

DIFFaX Calculations. Planar faulting in crystals leads to index-dependent peak widths and diffuse scattering contributions in powder diffraction. In this study, the DIFFaX v1.812 software was used to simulate X-ray powder diffraction patterns of stacking-disordered ice structures (19). Structural information required by DIFFaX includes the cell dimensions, details of the atoms within the cells, the interlayer stacking vectors, and the stacking transitions probabilities (φ_{ij}, see below). DIFFaX makes use of a recursion algorithm, which builds on the self-similarity present in ordered as well as random stacking sequences. The total diffracted intensity from a statistical ensemble of crystallites is then calculated from the incoherent sum of the diffraction arising from each crystallite orientation and defect arrangement. Peak broadening due to finite crystallite size and instrumental parameters is treated phenomenologically by DIFFaX. In a last step, the calculated intensities are convoluted with profile functions, such as Gaussian functions, which we used in this study.

Definition of the Stacking Probability Ratio $\Phi_c:\Phi_h$. The stacking disorder in ice is defined using the $\Phi_c:\Phi_h$ notation that can describe any combination of stacking probabilities. Φ_c is defined as the probability (expressed as a percentage) of a hexagonal sequence transitioning (or faulting) to a cubic sequence, and therefore $100 - \Phi_c$ is the probability of continuing in a hexagonal sequence. Φ_h is the probability of a cubic sequence transitioning to a hexagonal sequence and accordingly the probability of remaining in a cubic sequence is $100 - \Phi_h$.

In DIFFaX, the stacking transition probability is defined as φ_{ij}, which denotes the probability of a stacking transition from layer i to layer j (20). We use a model with four distinct layers which are defined in *SI Dataset*. The probability ratio is related to the stacking transition probabilities in the DIFFaX data file as follows:

$$\Phi_h = \varphi_{12} = \varphi_{43} \text{ (transitioning from a cubic to a hexagonal sequence);}$$
$$100 - \Phi_h = \varphi_{11} = \varphi_{44} \text{ (continuing in a cubic sequence);}$$
$$\Phi_c = \varphi_{24} = \varphi_{31} \text{ (transitioning from a hexagonal to a cubic sequence);}$$
$$100 - \Phi_c = \varphi_{23} = \varphi_{32} \text{ (continuing in a hexagonal sequence),}$$

which leads to a range of possible scenarios:

1. Random stacking, $\Phi_c + \Phi_h = 100\%$. A probability ratio of $\Phi_c:\Phi_h = 30\%:70\%$ would indicate a material with overall 30% cubic sequences and 70% hexagonal sequences randomly distributed through the structure [proportion cubic $= \Phi_c/(\Phi_c + \Phi_h)$]. In this example, there is a 30% chance of transitioning from a hexagonal sequence to a cubic sequence (Φ_c) and consequently also a 30% chance of continuing the cubic sequence ($100 - \Phi_h$). Hence, when $\Phi_c + \Phi_h = 100\%$, the probability of a particular sequence appearing is independent of the stacking history.
2. Stacking with memory effects or Reichweite, $\Phi_c + \Phi_h \neq 100\%$. Stacking history is known to play a role in determining stacking probability in some materials (20) and can manifest itself in several general groups of structures:

i. $\Phi_c < 50\%$, $\Phi_h < 50\%$. There is a low probability of a hexagonal sequence faulting to a cubic sequence, but when it does there is also a low probability of switching back to a hexagonal sequence. The resulting structure contains extended clusters of cubic and hexagonal sequences.
ii. $\Phi_c > 50\%$, $\Phi_h > 50\%$. Conversely, there may be a situation in which the probability of faulting is large, and frequent switching between hexagonal and cubic sequences will be observed. The limiting case is where $\Phi_c:\Phi_h = 100\%:100\%$, in which each cubic layer will be followed by a hexagonal layer and vice versa.
iii. $\Phi_c < 50\%$, $\Phi_h > 50\%$ or $\Phi_c > 50\%$, $\Phi_h < 50\%$. In these cases, there is greater probability of remaining in either a hexagonal or cubic sequence.

Monte Carlo Simulations. MC simulations were carried out in the isothermal-isobaric (pressure = 1 bar) ensemble for a system of 2,880 water molecules with the use of the TIP4P model. We employed the well-known umbrella sampling method coupled with an order parameter based on the recently developed maximum projection method (28) in order to enhance ice crystal growth. The maximum projection order parameter is capable of efficiently directing the growth of both ice forms, I_c and I_h, without an undesirable preference of either symmetry. As a result, this scheme allows the two ice sequences to emerge and grow competitively at the same time, which in all our simulations yields structures consisting of approximately randomly stacked cubic and hexagonal layers.

A strong biasing potential with respect to a quality-weighted ice cluster size, q, was imposed with an incline toward its higher values. At a given temperature, parallel simulations were performed for a number of system replicas restricted to parameter "windows" spanning a range of $q = [0,\ldots,0.1]$, which corresponded to the overall ice fraction of up to approximately 10%. In comparison to the results reported by Brukhno et al. (28), a significantly larger system ($N = 2{,}880$ vs. 768 and 360 water molecules) has been simulated.

Several simulations for the system of 2,880 water molecules have been performed at $T = 220$ K and the MC trajectories comprised up to 10^6 sweeps (a sweep corresponds to one translation or rotation attempt for every molecule in the system). The size of the ice cluster reached up to 200–300 water molecules.

ACKNOWLEDGMENTS. We thank A. Bertram for valuable discussions and J. Marsham and T. Wilson for critically reading the manuscript. We also thank C. Kilner for his assistance in running the X-ray diffractometer. The experimental aspects of this study were funded by European Research Council (FP7, 240449 ICE), and the molecular simulations were partly supported by Engineering and Physical Sciences Research Council (GR/T27112/01).

1. Murray BJ, Bertram AK (2008) Inhibition of solute crystallisation in aqueous H^+-NH_4^+-SO_4^{2-}-H_2O droplets. *Phys Chem Chem Phys* 10:3287–3301.
2. Murray BJ, Knopf DA, Bertram AK (2005) The formation of cubic ice under conditions relevant to Earth's atmosphere. *Nature* 434:202–205.
3. Murray BJ, Bertram AK (2006) Formation and stability of cubic ice in water droplets. *Phys Chem Chem Phys* 8:186–192.
4. Mayer E, Hallbrucker A (1987) Cubic ice from liquid water. *Nature* 325:601–602.
5. Murphy DM (2003) Dehydration in cold clouds is enhanced by a transition from cubic to hexagonal ice. *Geophys Res Lett* 30:2230, 10.1029/2003GL018566.
6. Murray BJ, Jensen EJ (2010) Homogeneous nucleation of amorphous solid water particles in the upper mesosphere. *J Atmos Sol Terr Phys* 72:51–61.
7. Murray BJ, Plane JMC (2005) Uptake of Fe, Na and K atoms on low-temperature ice: Implications for metal atom scavenging in the vicinity of polar mesospheric clouds. *Phys Chem Chem Phys* 7:3970–3979.
8. Murray BJ, Plane JMC (2003) Atomic oxygen depletion in the vicinity of noctilucenit clouds. *Adv Space Res* 31:2075–2084.
9. Dubochet J, et al. (1988) Cryo-electron microscopy of vitrified specimens. *Q Rev Biophys* 21:129–228.
10. Mehl P, Boutron P (1988) Cryoprotection of red blood cells by 1,3-butanediol and 2,3-butanediol. *Cryobiology* 25:44–54.
11. Furukawa Y (1982) Structures and formation mechanisms of snow polycrystals. *J Meteorol Soc Jpn* 60:535–547.
12. König H (1943) A cubic ice modification (Translated from German). *Z Kristallogr* 105:279–286.
13. Petrenko VF, Whitworth RW (1999) *Physics of Ice* (Oxford Univ Press, Oxford), pp 276–277.
14. Kohl I, Mayer E, Hallbrucker A (2000) The glassy water-cubic ice system: A comparative study by X-ray diffraction and differential scanning calorimetry. *Phys Chem Chem Phys* 2:1579–1586.
15. Arnold GP, Finch ED, Rabideau SW, Wenzel RG (1968) Neutron-diffraction study of ice polymorphs. III. Ice I_c. *J Chem Phys* 49:4365–4369.
16. Hansen TC, Koza MM, Kuhs WF (2008) Formation and annealing of cubic ice: I. Modelling of stacking faults. *J Phys Condens Matter* 20:285104.
17. Kuhs WF, Bliss DV, Finney JL (1987) High-resolution neutron powder diffraction study of Ice-I_c. *J Phys Colloq* 48:631–636.
18. Morishige K, Yasunaga H, Uematsu H (2009) Stability of cubic ice. *J Phys Chem C* 113:3056–3061.
19. Shilling JE, et al. (2006) Measurements of the vapor pressure of cubic ice and their implications for atmospheric ice clouds. *Geophys Res Lett* 33:L17801:1–5.
20. Treacy MMJ, Newsam JM, Deem MW (1991) A general recursion method for calculating diffracted intensities from crystals containing planar faults. *Proc R Soc Lond A* 433:499–520.
21. Elarby-Aouizerat A, Jal J-F, Dupuy J, Schildberg H, Chieux P (1987) Comments on the ice I_c structure and I_c to I_h phase transformation mechanism : A neutron scattering investigation of ice precipitates in glassy $LiCl{\cdot}D_2O$. *J Phys Colloq* 48:C1-465–470.

22. Hansen TC, Koza MM, Lindner P, Kuhs WF (2008) Formation and annealing of cubic ice: II. Kinetic study. *J Phys Condens Matter* 20:285105.
23. Dowell LG, Rinfret AP (1960) Low-temperature forms of ice as studied by X-ray diffraction. *Nature* 188:1144–1148.
24. Jenniskens P, Banham SF, Blake DF, McCoustra MRS (1997) Liquid water in the domain of cubic crystalline ice I_c. *J Chem Phys* 107:1232–1241.
25. Pusey PN, et al. (1989) Structure of crystals of hard colloidal spheres. *Phys Rev Lett* 63:2753–2756.
26. Weiss Z, Capkova P (1999) Effect of stacking disorder on the profile of the powder diffraction line. *Defect and Microstructure Analysis by Diffraction*, eds R Snyder, J Fiala, and HJ Bunge (Oxford Univ Press, New York), pp 318–329.
27. Anwar J, Zahn D (2011) Uncovering molecular processes in crystal nucleation and growth by using molecular simulation. *Angew Chem Int Ed* 50:1996–2013.
28. Brukhno AV, Anwar J, Davidchack R, Handel R (2008) Challenges in molecular simulation of homogeneous ice nucleation. *J Phys Condens Matter* 20:494243.
29. Carignano MA (2007) Formation of stacking faults during ice growth on hexagonal and cubic substrates. *J Phys Chem C* 111:501–504.
30. Pirzadeh P, Kusalik PG (2011) On understanding stacking fault formation in ice. *J Am Chem Soc* 133:704–707.
31. Pluhařová E, Vrbka L, Jungwirth P (2010) Effect of surface pollution on homogeneous ice nucleation: A molecular dynamics study. *J Phys Chem C* 114:7831–7838.
32. Whalley E (1981) Scheiner's halo: Evidence for ice I_c in the atmosphere. *Science* 211:389–390.
33. Lawson RP, et al. (2008) Aircraft measurements of microphysical properties of subvisible cirrus in the tropical tropopause layer. *Atmos Chem Phys* 8:1609–1620.
34. Ulanowski Z, Kaye PH, Hirst E, Greenaway RS (2010) Light scattering by ice particles in the Earth's atmosphere and related laboratory measurements. *12th International Conference on Electromagnetic and Light Scattering*, eds K Muinonen, A Penttilä, H Lindqvist, T Nousiainen, and G Videen (University of Helsinki, Helsinki), pp 294–297.
35. Keyser LF, Leu MT (1993) Surface-areas and porosities of ices used to simulate stratospheric clouds. *J Colloid Interface Sci* 155:137–145.
36. Goodman J, Toon OB, Pueschel RF, Snetsinger KG, Verma S (1989) Antarctic stratospheric ice crystals. *J Geophys Res Atmos* 94:16449–16457.
37. Riikonen M, et al. (2000) Halo observations provide evidence of airborne cubic ice in the Earth's atmosphere. *Appl Optics* 39:6080–6085.
38. Murray BJ, et al. (2010) Kinetics of the homogeneous freezing of water. *Phys Chem Chem Phys* 12:10380–10387.

Correction

EARTH, ATMOSPHERIC, AND PLANETARY SCIENCES

Correction for "Structure of ice crystallized from supercooled water," by Tamsin L. Malkin, Benjamin J. Murray, Andrey V. Brukhno, Jamshed Anwar, and Christoph G. Salzmann which appeared in issue 4, January 24, 2012, of *Proc Natl Acad Sci USA* (109:1041–1045; first published January 9, 2012; 10.1073/pnas.1113059109).

The authors wish to note the following: "We would like to draw attention to the work of Molinero and co-workers (1, 2), which is relevant for our article. Moore and Molinero (2) very recently conducted a large scale molecular dynamics study into the structure of ice that crystallizes at 180 K. They find that the ice that forms in their simulations contains both cubic and hexagonal sequences with a ratio of about 2:1, similar to their previous study on ice formation in a nanopore (1). This work supports our conclusion that the material referred to as cubic ice in the literature is actually stacking disordered ice, but our experiments and simulations indicate that the ratio of cubic to hexagonal sequences is not restricted to 2:1."

1. Moore EB, de la Llave E, Welke K, Scherlis DA, Molinero V (2010) Freezing, melting and structure of ice in a hydrophilic nanopore. *Phys Chem Chem Phys* 12:4124–4134.
2. Moore EB, Molinero V (2011) Is it cubic? Ice crystallization from deeply supercooled water. *Phys Chem Chem Phys* 13:20008–20016.

www.pnas.org/cgi/doi/10.1073/pnas.1201020109